MOMENTUM SLITS, COLLIMATORS AND MASKS IN THE SLC*

D. R. Walz, A. McFarlane, E. Lewandowski and J. Zabdyr

Stanford Linear Accelerator Center, Stanford University, Stanford, California 94309

ABSTRACT

The high specific power densities in the SLC give rise to a multitude of challenging problems in collimation and momentum analysis, beam containment, machine protection and background control. The results of an extensive program to develop most of the devices deemed necessary for operation of the arcs matching sections and the final focus region are presented. Emphasis is placed on materials selection and on unique features of remotely adjustable slits and halo clipper collimators which have to operate with great precision in a high-radiation, ultra-high vacuum environment. Also covered are solutions for a few fixed aperture machine protection collimators.

1. INTRODUCTION

The Final Focus System (FFS) of the SLC stretches over a distance of ~300 m. It contains some 200 dipoles, quadrupole and sextupole electromagnets. Interspersed between them are about 140 beam-diagnostic instruments and collimators. Some magnets are operated in series from a single power source, whereas others are powered by their own dedicated supply. This fact plus the possibility of magnet failure, human error and wrong launch conditions from the collider arcs, when coupled with the large specific current density of SLC bunches, necessitated development of an extensive machine protection system. The implementation of such a scheme was complicated by the fact that, after colliding at the interaction point (IP), the "spent" bunches are transported to their respective beam dumps through the transport system of the opposite polarity. If the momenta of the electron and positron bunches differ (and they may by $\leq 2\%$) the trajectories of the incoming (primary) and spent beams will not coincide. Finally, if the RF bunches contain the nominal number of $e^{\pm}$ and are properly focused at the IP, then the two bunches are "disrupted" and will leave the IP with angular divergences which are larger than those predicted for one bunch only.

The apertures of transport magnets and instruments as well as those of the interconnecting vacuum drift chambers had to be made large enough to allow passage of these bunches without excessive losses. At the worst, the latter can result in destruction of beam transport components and generation of unwanted residual radioactivity. Even if the hardware survived the unscheduled targeting of such bunches, the resulting secondaries (e, γ, μ, n, etc.) might prove to be excessive background for successful operation of the detector at the IP. Transverse dimensions of 10σ and 3σ for primary and disrupted (spent) beams were used as a compromise to define the beam stay-clear envelope.[1,2] The initial goal was to specify and implement a machine protection scheme (MPS) in the form of fixed aperture protection collimators (PCs) interspersed between the optical elements and diagnostic instruments which would protect against all known exposure hazards.

As the various sources of background harmful to the detector were identified and quantified it became evident that additional adjustable background-reducing clippers and masks were required. In some cases beam axial space was so tight that background reduction and MPS functions had to be combined into one device. As a consequence of these considerations a collimation scheme was implemented consisting of some 100 x- and y-adjustable collimators, x-adjustable momentum slits, and fixed aperture PCs.

2. COLLIMATION AND POWER ABSORPTION MEDIUM

The heart of each collimator, mask or slit is the power absorption medium. Ideally, the material should be high-Z with sufficient longitudinal and transverse thickness to completely attenuate and absorb the electromagnetic cascade shower which results from targeting of multi-GeV $e^+/e^-/\gamma$. Further, it is desirable that the full beam can be targeted indefinitely. Unfortunately, the small transverse beam dimensions of the SLC, when coupled with the high single-bunch charge, result in local peak power densities which are detrimental to all but the lowest-Z engineering materials available.

The pertinent beam parameters for this task were: $E_o = 50$ GeV, $N = 5 \times 10^{10}$ e/bunch, PRR = 180 Hz, with resultant single bunch energy of 400 J and an average power of 72 kW. These are coupled to an invariant emittance of the SLC linac of $\gamma\epsilon = 3 \times 10^{-5}$ mrad. Typical primary transverse beam sizes and other pertinent data are given in Table 1 for a selected list of collimators. The order is from the end of the linac toward the IP.

Table 1 Typical Final Focus Collimators and Beam Sizes

Device ID	Beam Size σ_x	Beam Size σ_y	Adopted $\frac{1}{2}$ Aperture	Absorber Depth X_o	Mtl(s)	Function
	–	μm	μm	mm	–	–
SL-1	160	110	-3 to 12.7	3.8/9.8	Ti/Cu	x-a
SL-2	200	90	-3 to 12.7	40	Cu/Cu-Al/W	x-a
SL-9	120	120	0 to 12.7	3.8/9.8	Ti/Cu	x,y-a
PC-19	55	50	2.0	4.0	Ti/Cu	f
PC-18	70	230	3.2 to 5.0	4.7	Ti/Cu	f
CIX-MKI	130	350	0.75 min	4.0	Ti/Cu	x-a/f
-MKII	130	350	0.75 min	24	W/Cu	x-a/f
PC-B3	75	75	3.4	2.7	Ti/Cu	f
PC-12 -MKI	1090	290	1.2 to 6	3.8/9.8	Ti/Cu	x, y-a
-MKII	1090	290	1.2 to 16	40/20	W/W-Cu	x, y-a
PC-6.5	300	220	7.1	10.5	Cu	f
PC-6	310	310	38.1	20.2	Cu	f
PC-3	1420	790	5 to 25	40/20	W/W-Cu	x,y-a
M1	1550	870	17.5	26.5	Ta	f

a – adjustable aperture f – fixed aperture

Extensive simulations of cascade showers were carried out using the Monte Carlo computer code EGS. Materials which received special attention were W-25Re, Ta-10W, free-machining tungsten (~90% W), Cu, INVAR, 18-8 stainless steel, two titanium alloys, aluminum, and aluminum oxide. Of primary interest were the single-bunch temperature increase and the resulting thermal stress rise. In the SLC the bunch length is 1-2 ps and the heated volume will have essentially reached its maximum temperature at the end of this time interval. In the worst case, the heated volume will have melted in one bunch. Otherwise, the consequence of this temperature spike will be the generation of instantaneous compressive thermal stresses and strains. If the stress gradients are steep enough a pressure or shock wave will begin propagating at velocity of sound in the local medium. When reflected on free surfaces or discontinuities these compression waves will cause tensile stresses and perhaps failure by spallation if material limits are exceeded. Certain unfavorable surface geometries can cause shock focusing, thereby enhancing the detrimental effects. Shock physics experiments[3] demonstrated that an instantaneous tensile stress rise equal to or in excess of four times the ultimate tensile strength σ_{ut} of the material will cause fracture or spallation for a single exposure.

* Work supported by the Department of Energy contract DE-AC03-76SF00515.

CH2669-0/89/0000-0553$01.00©1989 IEEE

Such a material failure occurred on a tungsten target[4] using a SLAC pulse with a width of ~1.6 μs.

For stress intensities below those causing instant catastrophy multiple exposures with consequential plastic strain determine the life expectancy of a target. Pulsed accelerators such as SLAC accumulate large numbers of exposures in a short time, and target designs must be tailored to the endurance limit of the materials. Such multiple exposures from a train of bunches also cause a steady state temperature and thermal stress distribution onto which the individual bunch temperature and stress spikes are superimposed. The shower simulations convincingly showed that for the aforementioned beam parameters high-Z collimators are only feasible if the transverse beam size is $\sigma \geq 1$ mm. In the SLC FFS the beam is this large only in the final transformer at mask M–1 and PC–3. Everywhere else transverse beam sizes are more like ~ 200 μm and in some locations much less than that. For $\sigma = 200$ μm the maximum single bunch temperature rise in a volume element of $0 < r \leq 100$ μm in a semi-infinite medium of W–25 Re was found to be $\Delta T \sim 2800°$. It occurred at a depth of ~6 radiation lengths (X_o) which is somewhat less than the $\sim 8X_o$ predicted for shower maximum. This results from the transverse spread of the shower due to multiple scattering which, at that depth, begins to dominate the still rising shower population. While it would take $\sim 6 \times 10^{10}$ e/bunch to melt this material, the consequences of this exposure are just as disastrous at 5×10^{10}. The resulting thermal stress rise in a fully restrained body is $\sigma_{th} \propto E\alpha\Delta T$. It is of the order of 7×10^8 $Pa(10^5\text{psi})$ (where E is the modulus of elasticity and α is the linear coefficient of thermal expansion; both are assumed not to vary with temperature for this exercise). This is in excess of $4\sigma_{ut}$ for this material at room temperature; it is also $\sim 15\sigma_{end}$, the endurance limit. The other high-Z materials showed similar values, namely $\sim 3000°, \sim 2500°$ and $\sim 2000°$ for W–5Ir, Ta–10W and free-machining tungsten, respectively. Copper showed a temperature spike of 375° and resulting stress rise of $\sim 8.3 \times 10^8$Pa (1.2×10^5psi), which is $\sim 3.7\sigma_{ut}$ and $\sim 15\sigma_{end}$.

A relative measure of a material's worth can be obtained from the quantity $E\alpha\Delta T/\sigma_{ut}$. Titanium and its alloys compared very favorably to other materials. The maximum single bunch temperature rise in Ti–6Al–4V is of the order of 130–140° with a corresponding thermal stress rise of $\sim 1.3 \times 10^8$Pa (1.9×10^4 psi) this is $\sim 0.14\sigma_{out}$ and $0.25\sigma_{end}$. The iron-nickel alloy INVAR appeared promising due to its very low α. Unfortunately, the latter increases dramatically above ~ 175°. Steady state operating conditions could be far higher because of its poor thermal conductivity. High-purity aluminum oxide (Al_2O_3) also had some appeal, particularly its high melting point and compressive strength. Its low elongation coupled to a high E, namely brittleness, in combination with low tensile strength makes it a poor choice for thermal shock exposure; further, it is a dielectric, and fractures have occurred from spontaneous discharge. Aluminum has poor elevated temperature properties offsetting its otherwise moderate potential. Last, beryllium and carbon (graphite) had too many handicaps for serious consideration.

Thus titanium, particularly the alloys Ti–6Al–4V, Ti–5Al–2.5Sn and Ti–6Al–6V–2Sn emerged as clear candidates for these applications. If it were not for their low thermal conductivity, they would be nearly perfect materials. The decision was made to utilize titanium in all but those few locations where the predicted beam size is large enough to use either high-Z materials or copper. All collimator jaws were made as thin as possible in the transverse dimension, consistent with the maximum predicted lateral beam excursion and radial shower spread. The Ti-jaw module is then backed by a slab of copper to which a heat sink is attached.

Selection of an optimal longitudinal jaw depth proved to be more difficult. To minimize leakage of secondaries emerging from the downbeam jaw face with sufficient momentum to be transported to the vicinity of the detector and also to protect nearby equipment, the jaw should be as long as possible. To minimize secondaries being scattered out of the front or collimating face the jaw should be made as short as possible. Shower studies showed that the jaws need to be at least $3X_o$ long. Results were independent of Z when plotted in units of X_o. The low thermal conductivity of titanium set an upper limit on jaw length for continuous beam exposure, well short of shower maximum. Approximately $4X_o$ proved to be an all-around compromise.

The orientation of the jaw collimating faces relative to beam direction also received scrutiny. It was demonstrated[5] that background increased if the beam impinged onto the collimating face, reaching maximum for a jaw rotation 250–300 μrad. The same investigation also showed that jaw rotation in the opposite direction with resultant beam impingement on the upbeam endface increased leakage through the front or collimating face, thereby increasing background but eventually leveling off beyond a rotation of 1 mrad. It was suggested[5] and verified with EGS that the addition of a thin layer (~10–20 μm thick) of a high-Z material (Au) to the collimating face would cause the slit-scattered secondaries to loose additional energy and render most of them harmless for background generation at the IP. Last, it was proposed[6] that making the collimating face mildly convex would desensitize the jaw rotational alignment tolerance (pitch and yaw) and reduce background. This was modeled[5] with EGS and a broad minimum was found for radii in the range from 7–12 m. The power absorbing jaws have their leading and trailing edges radiused (r = 3 mm) to prevent increase in the wakefield function when the jaws operate in very close proximity of the beam.

3. A TYPICAL x,y–ADJUSTABLE COLLIMATOR

The following is a set of criteria which the adjustable collimators had to meet: (1) each slit consists of two opposing jaws; (2) each jaw is independently adjustable or can move in unison with the opposing jaw; (3) upbeam and downbeam ends of a jaw can be driven independently or together; (4) each horizontally collimating jaw is able to overtravel the nominal beam centerline by 3 mm; (5) the drive system has no backlash; (6) each collimator is self-calibrating via built-in fixed datum reference points; (7) each jaw is water cooled; (8) collimators are built for ultra-high vacuum application; (9) cooling loops are continuous, without water-to-vacuum joints; (10) collimators are capable of operating in a high-radiation environment; (11) each jaw has a secondary emission monitor (SEM) foil (Ti) mounted to its upbeam face; and (12) the vacuum has no bearings or friction surfaces.

All adjustable collimators were cloned from this basic package to have a high degree of interchangeability of parts. Deviations from it reflect specific local requirements. For example, in some slits the opposing jaws are coupled together and move symmetrically about a nominal centerline without possibility of zero overdrive. The introduction of the convex jaw surface and consequential relaxation of rotational tolerances allowed coupling of upbeam and downbeam ends and operation from one prime mover. Backlash in the drives was eliminated by using ball screw shafts with double ball-nuts and preloading. Figure 1 shows a typical jaw assembly outside its vacuum chamber. All hardware is mounted to a flange. The jaws are hanging from torsion bar supports which operate in bending and torsion. They allow front-rear differential adjustment without having any bearings or other sliding surfaces in the vacuum. These torsion bars are attached to horizontal shafts for support and adjustment. All external bearings and friction surfaces were dry-coated with tungsten disulfide (WS_2) in order to operate unlubricated if necessary. They were, however, additionally coated with a mixture of a silicone oil and molybdenum disulfide (MoS_2) to further reduce the coefficient of friction.

The prime mover is a stepping motor with 400 steps/revolution. Drive shaft and ball nut have a lead of 5 mm/revolution. Thus, one step corresponds to a linear jaw travel of 12.5 μm. The position of each jaw is monitored by a linear variable differential transformer (LVDT). The extremes of travel are monitored by limit switches which are protected against excessive overtravel by built-in adjustable limits. Collimators with centerline overtravel have floating limit switches. The Ti-jaw dimensions are $\sim 8 \times 120 \times 140$ mm. The average power deposited in a $3.8X_o$ long jaw at 10 Hz is 275 W. The resulting maximum steady

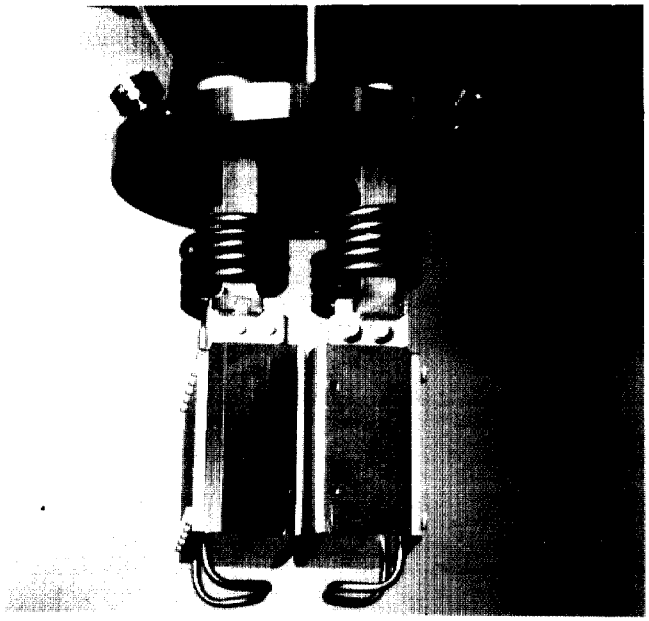

Fig. 1: Titanium/copper slit jaw assembly

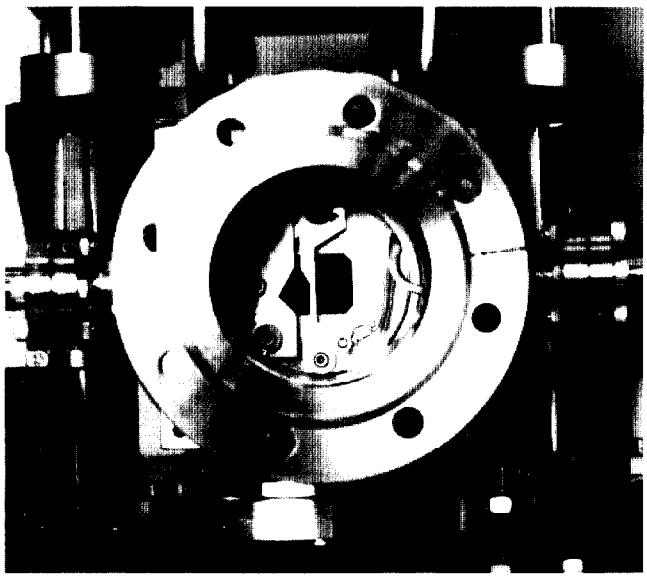

Fig. 2: End view of C1X fork collimator

state temperature difference to the water is $\sim$ 500° and was computed using the two-dimensional computer code POISSON. Single bunch temperature spikes are $\sim$ 170°. Cooling is by low-conductivity water (LCW, $\geq 10^6\Omega$ cm). The mass flow rate is $\sim$0.06 l/s (1 gpm) for a slit (two jaws in series) at a maximum supply temperature of $\sim$ 30°. The corresponding velocity is $\sim$3.4 m/s and the bulk temperature rise is 1° per jaw. The flow is interlocked by a differential pressure switch. Temperatures are monitored with immersion-type platinum resistance temperature detectors (RTDs).

The convex collimating jaw surface (r = 10 m) was generated by wire electric discharge milling (EDM) to an accuracy of $\sim 10\ \mu$m. A second clean-up cut was necessary to achieve the desired surface finish of $\leq 1.5\ \mu$m. This reflects the fact that only particles impinging within $\leq 2\ \mu$m from the surface contribute to harmful scattered flux. The curved section is $\sim$100 mm long and is followed on either end by a 20-mm-long tapered section at an angle of 10°. The backup copper slab is $\sim$55 mm wide and also has a curved front surface, normal to the beam direction. This is to guarantee longterm good thermal contact for the flat titanium plate in the area closest to beam impingement. Titanium and copper slabs are bolted together since brazing of the two materials is problematical due to formation of brittle intermetallic constituents.

The location of the geometric center of these devices was referenced and encoded to tooling balls attached outside on the main mounting flange. Encoding was done with a coordinate measuring machine (CMM). The goal was to know the transverse locations of the slit jaws to an accuracy of $\pm 100\ \mu$m relative to the local beam survey line, and to ± 1 mm in beam direction. The rotational tolerances are 0.5 mrad for pitch and yaw, 10 mrad for roll.

The last clipper collimator before the IP, PC-3, is exposed to beams with $\sigma \sim 1$ mm. This enabled the use of free-machining tungsten for the front face of the jaws with a length of $\sim 40X_o$ to a transverse depth of 11 mm, and $\sim 20X_o$ beyond 11 mm. The jaw is thus a complete shower attenuator, absorbing $\sim$ 4 kW at10 Hz. The Ti-jaws in PC-12 (x, y) and C1Y were temporarily replaced by tungsten jaws as in PC-3 to further reduce background to the IP during early low-intensity ($\sim 10^{10}e$/bunch) commissioning.

Simulations using the computer code TURTLE showed that the location of the C1 collimator in the outer transformer was particularly suitable for removal of background-generating $e^{\pm}$. This device is located beyond the point where the extraction line kicker magnet deflected the spent beam (by 1.2 mrad) from the primary beam trajectory. The two beams are separated by $\sim$8 mm. This made it impossible to utilize one of the previously described slits for x-collimation. The y-slit was made into a separate unit. The x-slit became simultaneously a halo clipper on the primary beam and a protection collimator for a quadrupole magnet on the extracted beam. An end view of this device is shown in Fig. 2, and Fig. 3 depicts the overall assembly. Change of slit opening or width of cut on the primary beam is accomplished by means of a tapered slot varying in width from 1.5–6 mm. The whole assembly is translated vertically and in the fully "out" position it offers a wide area for beam studies. The first generation device consisted of a $4X_o$ long titanium cylinder imbeded in a copper block (tapered shrink fit). This unit was temporarily replaced by one having a $24X_o$ long tungsten insert to aid in commissioning. Background is minimized by a stepping motor-controlled yaw adjustment with a single step corresponding to $\sim 12.5\ \mu$rad over a range of $\pm$ 1 mrad.

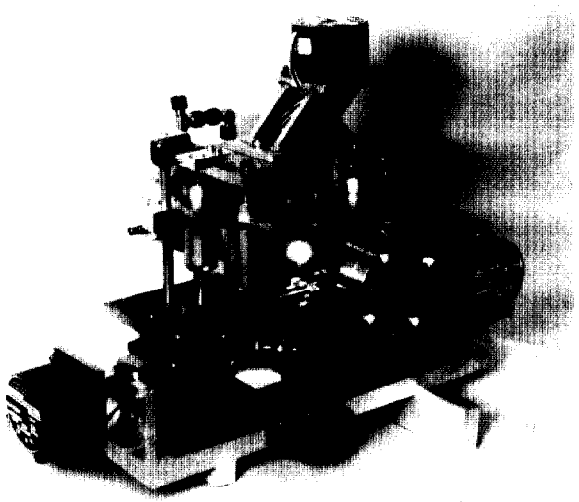

Fig. 3: C1X fork collimator assembly

5. MOMENTUM SLITS

A momentum-defining slit facility was installed in each of the two linac-to-arcs matching sections. The goal was to build devices which could withstand the consequences of individual bunches with $5 \times 10^{10} e$ and which, when fully closed, could also be used to park and dissipate the full beam (72 kW at 180 Hz) indefinitely. In order to achieve good momentum resolution (0.056%) a location was selected some 30 m downbeam of the end of the linac, where the eta-function is large and the beta-function is relatively small. There, the nominal transverse dimensions of the beam are $\sigma_x \sim 150$ μm and $\sigma_y \sim 120$ μm which forced a separated function design. The first slit, SL–1, is of the titanium jaw variety as described under (3) above. It is *the* momentum slit and at the same time a "spoiler" which, by multiple coulomb scattering, increases the beam spot to a size that results in manageable single-bunch temperature spikes at the second device, SL–2, located ~1.3 m downbeam. The latter is only a residual power absorber, but it can dissipate the full 72 kW if the beam spot is large enough. Slit SL–1 had to be at least $3X_o$-long in order not to increase background at the detector located some 1400 m downbeam[2]. The jaws were made $\sim 4X_o$ long which leaves a residual of ~ 0.92 P_{av} for SL–2 at 50 GeV. With the exception of size and jaw design, this device incorporates some of the same features as SL–1. The jaws are hollow copper cylinders which contain a water-cooled packed bed of ~1-cm-diameter spheres.[7] The latter are made of copper-plated alumium in the region of shower maximum and of pure copper before and after. A block of tungsten was attached to the downbeam end of the module to more efficiently attenuate the cascade shower. The overall length is $40X_o$. The nominal flow rate is $\sim 0.6 l H_2O/s$ (10 gpm); at 72 kW, $\Delta T \sim 27$°C. An SL–2-type slit assembly is shown in Fig. 4.

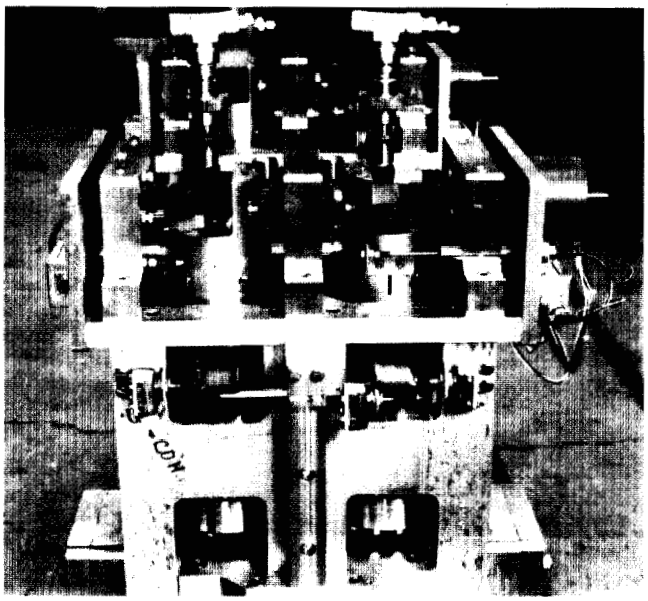

Fig. 4: SL–2-type split assembly

Unfortunately, this facility has one shortcoming, namely SL–1 is also limited to a steady state bunch rate of 10 Hz at 5×10^{10} e/bunch for the reasons previously presented. Yet it is highly desirable to accomodate 180 Hz in this facility, and a program is underway at this time to add a second spoiler ahead of SL–1. This device would only be inserted when SL–1 is in the "fully out" position and beams are to be parked, i.e. not transported to the IP. The spoiler then needs to be just long enough (1–1.5 X_o) to increase the beam spot to a size which results in manageable single bunch temperature spikes at SL–2.

6. FIXED APERTURE MACHINE PROTECTION COLLIMATORS

A large number of PCs were installed throughout the arcs matching-sections and the FFS to protect magnets, instruments, and vacuum chambers from direct exposure to the beam. Their basic design is shown in Fig. 5. The collimator body is copper ($\sim 10X_o$ long), peripherally water-cooled, with an aperture appropriate for the specific location. A titanium cylinder was imbeded into the Cu-body in those applications where $\sigma \leq 250$ μm. At mask M1, just ahead of the detector, where normally only a few stray particles are intercepted, the collimator is a 26.5 X_o-long tantalum cylinder, cooled peripherally by thermal radiation and natural convection only. At protection collimator PC–18 both the primary and the spent or extracted beam had to be accomodated in separate apertures in one device.

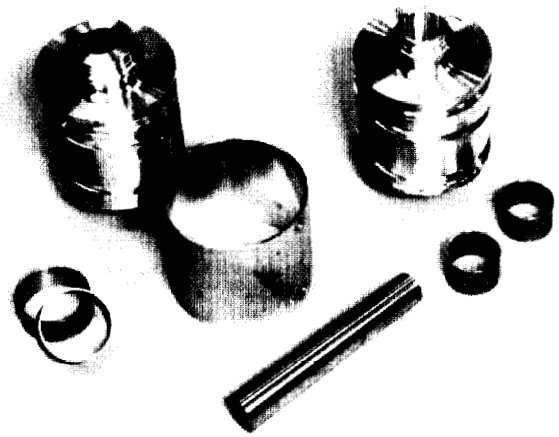

Fig. 5: Fixed aperture protection collimator parts

ACKNOWLEDGMENTS

The authors thank the members of the masking and collimators study group, especially D. Burke, H. DeStaebler, G. Fischer, L. P. Keller, W. Kozanecki and J. A. Mathews for their interest and contributions to this program. A debt of gratitude is also owed to L. Alton and B. Brugnoletti, who were the senior designers on the adjustable slits and collimators; to C. Perkins who coordinated many of the assembly and installation activities; and to M. Pan and the Editorial Services Department who prepared this manuscript.

REFERENCES

1. L. P. Keller, SLAC, private communication.
2. W. Kozanecki, SLAC, private communication.
3. D. R. Curran, SRI International, private communication.
4. D. R. Walz et al, "Tests and description of beam containment devices and instrumentation - A new dimension in safety "problems" IEEE Trans. Nucl. Sci. Vol. **NS–20**, No. 3, 465–470 (June 1973).
5. H. DeStaebler, SLAC, private communication.
6. G. von Holty, CERN, private communication.
7. D. R. Walz and L. R. Lucas, "The 'sphere dump' - a new low-cost high-power beam dump concept and a catalytic hydrogen-oxygen recombiner for radioactive water systems", IEEE Trans. Nucl. Sci. Vol. **NS–16**, No. 3, 613–617 (June 1969).